Radiological Physics and Technology (2021) 14:288–296
https://doi.org/10.1007/s12194-021-00626-2

Correlations between cardiovascular parameters and image parameters on dynamic chest radiographs in a porcine model under fluid loading

Rie Tanaka[1] · Tohru Tani[2] · Atsushi Yamada[2] · Soichiro Tani[3] · Khiem Tran Dang[2] · Norihisa Nitta[4] · Takahisa Tabata[5] · Shintaro Muraoka[6] · Tsutomu Yoneyama[6] · Shigeru Sanada[7]

Received: 13 February 2021 / Revised: 1 June 2021 / Accepted: 5 June 2021 / Published online: 21 June 2021
© Japanese Society of Radiological Technology and Japan Society of Medical Physics 2021

Abstract

Latest digital radiographic technology permits dynamic chest radiography during the cardiac beating and/or respiration, which allows for real-time observation of the lungs. This study aimed to assess the capacity of dynamic flat-panel detector (FPD) imaging without the use of contrast media to estimate cardiovascular parameters based on image parameters of a porcine model under fluid loading. Three domestic pigs were intubated, and mechanical ventilation was provided using a ventilator under anesthesia. A porcine model involving circulatory changes induced by fluid loading (fluid infusion/blood removal) was developed. Sequential chest radiographs of the pigs were obtained using a dynamic FPD system within the first 5 min after fluid loading. Image parameters such as the size of the heart shadow and mean pixel values in the lungs were measured, and correlations between fluid loading and cardiovascular parameters (blood pressure [BP], cardiac output [CO], central venous pressure [CVP], and pulmonary arterial pressure [PAP]) were analyzed based on freedom-adjusted coefficients of determination (R_f^2). Fluid loading was correlated with radiographic lung density and the size of the heart shadow. Radiographic lung density was correlated with the left and right heart system-related parameters BP, CO, CVP, and PAP. The size of the heart shadow correlated with the left heart system-related parameters CO and BP. Dynamic FPD imaging allows for the relative evaluation of cardiovascular parameters based on image parameters. This diagnostic method provides radiographic image information and estimates relative circulatory parameters.

Keywords Cardiovascular parameters · Circulation physiology · Dynamic chest radiology · Emergency medicine · Flat-panel detector

1 Introduction

Simple and rapid respiratory/circulatory examinations and imaging procedures are essential for treating critical patients during emergencies [1]. The cardiovascular parameters of seriously ill patients are usually monitored using invasive

This work originated from the Biomedical Innovation Center, Shiga University of Medical Science. Seta Tsukinowa-cho, Otsu, Shiga, 520-2192 Japan, for image acquisitions of animals, College of Medical, Pharmaceutical & Health Sciences, Kanazawa University. 5-11-80 Kodatsuno, Kanazawa, Ishikawa, 920-0942 Japan, for image analyses.

✉ Rie Tanaka
rie44@mhs.mp.kanazawa-u.ac.jp

[1] College of Medical, Pharmaceutical and Health Sciences, Kanazawa University, Kanazawa University, 5-11-80 Kodatsuno, Kanazawa, Ishikawa 920-0942, Japan

[2] Department of Research and Development for Innovative Medical Devices and Systems, Shiga University of Medical Science, Seta Tsukinowa-cho, Otsu, Shiga 520-2192, Japan

[3] Department of Surgery, Shiga University of Medical Science, Seta Tsukinowa-cho, Otsu, Shiga 520-2192, Japan

[4] Department of Radiology, Shiga University of Medical Science, Seta Tsukinowa-cho, Otsu, Shiga 520-2192, Japan

[5] Department of Critical and Intensive Care Medicine, Shiga University of Medical Science, Seta Tsukinowa-cho, Otsu, Shiga 520-2192, Japan

[6] Healthcare Business Headquarters, Konica Minolta, Inc., 2970 Ishikawa-machi, Hachioji, Tokyo 192-8505, Japan

[7] Clinical Engineering, Komatsu University, 10-10 Doihara-cho, Komatsu, Ishikawa 923-0921, Japan

pulmonary artery catheters (Swan-Ganz catheters), and their cardiac function is evaluated indirectly using a non-invasive echographic apparatus. Conventional chest radiography is also performed if necessary, for obtaining imaging information. In such an emergency setting, the recently developed dynamic chest radiography (DCR) can be a powerful tool for assessing cardiovascular conditions soon after admission to the emergency room, through the evaluation of dynamic imaging findings [2, 3].

The latest digital radiographic technology permits DCR during the cardiac beating and/or respiration, which allows for real-time observation of the lungs. The technology involves an imaging system that comprises a portable-type dynamic flat-panel detector (FPD) system (weight: 2–4 kg) and an X-ray generator capable of continuously generating X-ray pulses. With recent advances in FPD sensitivity, total radiation exposure can be less than the guidance levels for two projections recommended by the International Atomic Energy Agency (1.9 mGy) [4]. Dynamic chest radiographs contain abundant functional information, such as diaphragm movement, cardiac motion, pulmonary ventilation, and circulation [2]. In particular, there has been a major concern regarding circulation dynamics reflected as temporal changes in radiographic lung density, which are caused by relative changes in regional blood volume and vessel diameter in the lungs (Supplemental data) [5]. Previous studies have indicated that perfusion defects could be detected as decreased changes in radiographic lung density, even without the use of contrast media [6–8]. Pulmonary embolism (PE) has been reported to manifest as a mean reduction of 49.6% in temporal changes in radiographic density compared with temporal changes in an unaffected region, and as a mean reduction of 41.3% for the comparison between before/after the occurrence of PE in the same lung region [6]. Moreover, a high correlation was confirmed between the distribution of temporal changes in radiographic lung density and radioactivity counts on perfusion scintigraphy [7, 8]. The ejection fraction can also be derived from heart size and radiographic density [9]. Yamasaki et al. recently reported the use of DCR in detecting chronic thromboembolic pulmonary hypertension and pulmonary arterial stenosis in human subjects [10], while Hanaoka et al. demonstrated the ability of this technique to predict postoperative values and the risk of postoperative respiratory complications [11]. In addition, the feasibility of ventilation-perfusion studies based on changes in radiographic lung density has been demonstrated in clinical studies [12, 13]. These research findings indicate that DCR can be deployed as a simple and rapid means of functional imaging in both routine and emergency medicine, which demands ready access to such functional information. However, it is unclear whether DCR can quantify the increase and decrease in pulmonary blood volume as changes in radiographic lung density. In addition, it is unclear whether DCR can estimate cardiovascular parameters based on dynamic radiographic findings. It is necessary to address the relationship between cardiovascular parameters and image parameters on dynamic chest radiographs to implement DCR in emergency settings. On conventional chest radiographs, heart failure is generally characterized by cardiac hypertrophy and decreased radiolucency (i.e., increased lung density) in the lung fields [14, 15]. Therefore, we focused on cardiocirculatory changes in heart size and radiographic lung density on dynamic chest radiographs.

This study aimed to determine the correlation between cardiovascular and image parameters obtained using DCR. We demonstrate the results of a porcine study under fluid loading in which circulatory changes were induced by fluid infusion or blood removal.

2 Materials and methods

2.1 Animal preparation

Three female domestic pigs (body weight: 23–32 kg) were examined. The pigs were immobilized and placed in the supine position during the experiment and were intubated under inhalation anesthesia (Domitor, 1–3 μg) using a ventilator (COMPOS X; Metran Co., Ltd., Kawaguchi, Japan) (tidal volume: 300 mL/cycle, 15 cycles/min). The basic fluid infusion comprised lactated Ringer's solution and was intravenously administered at a rate of 60 mL/h.

Figure 1 shows the experimental procedure used in this study. We prepared porcine models involving circulatory changes induced by intravenous fluid infusion (saline infusion) or blood removal. In the infusion experiments (500 mL/session, over 6 min), the measurements were conducted in three to four periods: before loading (control level), after the initial infusion of 500 mL, after the second infusion of 500 mL (total: 1000 mL), and after the third infusion of 500 mL (total: 1500 mL). In the blood removal experiments (500 mL/session, over 5–10 min), the measurements were conducted across three periods: before blood removal, after removal of 500 mL of blood, and after further removal of 500 (or 200) mL of blood (total: 1000 or 700 mL). Here, the control level indicates the stable state of blood volume just before loading in each fluid loading (fluid infusion/blood removal) session. If an animal showed < 40 mmHg blood pressure (BP) and/or > 3.7 L/min/mm^2 cardiac output (CO), the data were excluded from the data analysis because the image parameters in such cases reached a plateau. Optimal loading conditions were determined based on the findings of our preliminary study aimed at keeping domestic pigs alive. Consequently, 6/21 image data from three animals were excluded according to the criteria above or due to erroneous imaging, and 15 images were analyzed in this study.

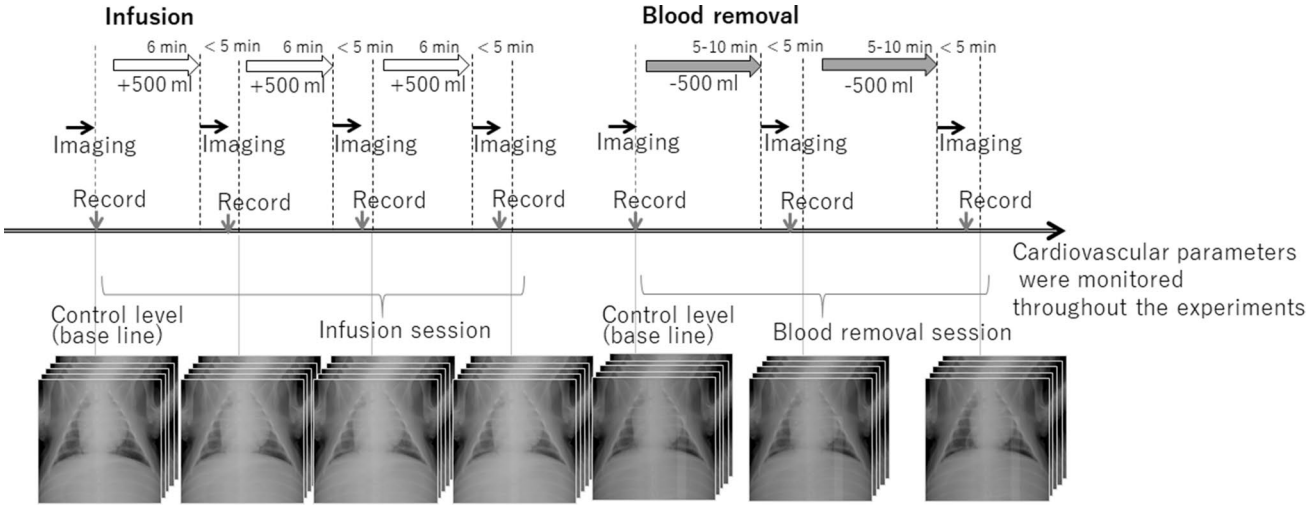

Fig. 1 Procedures for the infusion and blood removal experiments

The experimental protocol was approved by the Institutional Animal Care and Use Committee of our institution. All four domestic pigs were alive at the end of the study.

2.2 Measurement of cardiovascular parameters

Cardiocirculatory conditions were monitored throughout the experiment using a cardiovascular monitor (BSM-3000 cardiovascular monitor; Nihon Kohden, Tokyo, Japan), electrocardiogram (ECG) (Life Scope; Nihon Kohden, Tokyo, Japan), and a Swan-Ganz catheter (5Fr thermodilution catheter; Edwards Lifesciences Co., Ltd., CA, USA). One ECG electrode lead was placed on each of the forelegs and left hind leg. The catheter tip position was confirmed using X-ray fluoroscopy by a radiologist (N.N.) with 23 years of experience in interventional radiology. The cardiovascular parameters (BP [mmHg], CO [L/min/mm^2], central venous pressure [CVP, mmHg], pulmonary arterial pressure [PAP, mmHg], and heart rate [beats/min]), related to circulating blood volume and cardiac pumping function, were recorded within the first 5 min after circulatory loading to avoid the adaptive response of the body. We investigated the relationship between fluid loading and cardiovascular parameters to determine whether the porcine models showed normal circulatory reactions.

2.3 Imaging procedures

Sequential chest radiographs of the porcine models under fluid loading were obtained using a dynamic FPD imaging system (Test Model; Konica Minolta, Inc., Tokyo, Japan), comprising an indirect-conversion FPD (PaxScan, 4343CB; Varex Imaging Corporation, Salt Lake City, UT, USA), an X-ray tube (RAD-94/B-130H; Varian Medical Systems, Inc., Palo Alto, CA, USA), and an X-ray generator (Epsilon, EPS45RF; EMD technologies, Quebec, Canada). Imaging was performed within the first 5 min after circulatory loading (100 kV, 0.22 mAs/pulse, 15 frames/s, SID = 1.2 m) (Fig. 1). Respiration was suspended using a ventilator during imaging to exclude the influence of respiratory motion. A few images showed a slight motion of the diaphragm due to the failure of breath-holding, and such images were excluded from our image analysis. High linearity was confirmed between the detector's input X-ray dose and the output pixel values, whereby higher entrance doses to the detector were associated with higher pixel values. That is, decreased blood volume in the lungs reduces X-ray attenuation, resulting in increased radiographic lung density (indicated by black pixels), which is associated with higher pixel values in this study (Fig. 2). The matrix size was 1024 × 1024 pixels, the pixel size was 417 × 417 μm^2, and the gray-scale image range was 16 bits.

2.4 Measurement of image parameters

The size of the heart shadow and radiographic lung density were measured using an image analysis tool (Test Model; Konica Minolta, Inc., Tokyo, Japan) by a surgeon (T.T.). After adjusting the image contrast and brightness to improve the visibility of the lung and heart boundaries, the heart boundary was manually traced to measure the size of the heart shadow, whereas the lung density was calculated as the mean pixel value in both lungs. The measurements were performed on images at the end of the systolic phase in each cardiac phase showing the smallest heart size as well as the lowest radiographic lung density (Fig. 2), and the minimum value was selected for comparison with cardiovascular parameters. The average values from several

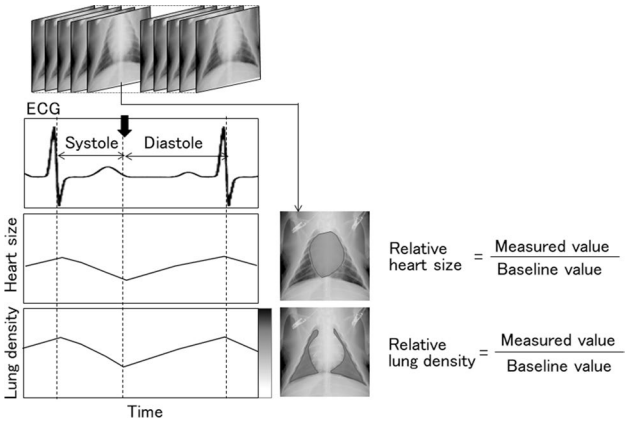

Fig. 2 Measurement of the image parameters. The black arrows indicate the timing and image frame for a particular measurement. The painted area indicates the size of the heart shadow and radiographic lung density. *ECG* electrocardiogram

images before fluid loading were used as baseline values. The relative increase in the size of the heart shadow and lung density compared with baseline values (measured using the initial images before fluid loading) was calculated in each animal to eliminate inter-individual differences in the image parameters.

2.5 Statistical analysis

Dependent relationships between the image parameters and cardiovascular parameters were evaluated using regression analysis (Microsoft Excel 2016; Microsoft Corp., WA, USA). The coefficient of determination (R^2) was used to determine the goodness of fit in a linear regression model. It is the square of the multiple correlation coefficient between the study and explanatory variables based on the sample values [16]. In this study, the resultant R^2 values were converted to degrees of freedom-adjusted coefficients of determination (R_f^2) owing to the relatively small number of cases. The degrees of freedom-adjusted coefficients of determination (corrected $R^2 = R_f^2$) were calculated using the following formula:

$$R_f^2 = 1 - (1 - R^2) \times \frac{N - 1}{N - P - 1}$$

where N is the sample size, P is the total number of explanatory variables in the model, and N–P–1 indicates the degrees of freedom. The terminology used to define the strength of the coefficients of determination is in accordance with [17]; coefficients of determination were considered to be weak when $R_f^2 \leq 0.12$, moderate when $0.12 < R_f^2 < 0.45$, and strong when $R_f^2 \geq 0.45$. An $R_f > 0.7$ was considered to indicate a high correlation [18].

3 Results

3.1 Circulatory reactions due to fluid loading

All porcine models subjected to fluid loading exhibited normal circulatory reactions. Figures 3 and 4 show the circulatory reactions to fluid infusion and blood removal in our porcine models. The coefficients of determination (R_f^2) for BP, CO, CVP, and PAP were 0.4873, 0.574, 0.722, and 0.343, respectively, and these cardiovascular parameters were correlated with the infusion load ($R_f = 0.700$, 0.758, 0.880, and 0.585, respectively) (Fig. 3). Similarly, the coefficients of determination (R_f^2) for BP, CO, CVP, and PAP were 0.908, 0.759, 0.849, and 0.703, respectively, and the parameters were highly correlated with blood removal ($R_f = -0.953, -0.871, -0.835$, and -0.921, respectively) (Fig. 4). We confirmed that our animal models were appropriate for evaluating the correlations between cardiovascular parameters and image parameters.

3.2 Relationship between fluid loading and image parameters

There was a correlation between image parameters and fluid loading (Table 1). The relative lung density indicated a highly negative linear correlation with the infusion load ($R_f = -0.820$) and a highly positive correlation with the blood removal load ($R_f = 0.978$) (Fig. 5). The relative heart size showed a high correlation with the blood removal load ($R_f = -0.932$) and a moderate correlation with the infusion load ($R_f = 0.444$) (Fig. 6). When the fluid load was restored to the control level, both image parameters returned to their initial levels. When the blood removed was returned to the porcine model, the circulatory parameters and mean pixel values returned to their initial levels.

3.3 Relationship between circulatory parameters and image parameters

The relationship between the examined cardiovascular parameters and image parameters obtained using DCR is shown in Figs. 7 and 8. The relative lung density correlated with the left and right heart system-related parameters BP ($R_f = 0.827$), CO ($R_f = 0.848$), CVP ($R_f = 0.737$), and PAP ($R_f = 0.731$) (Table 2). The relative heart size was correlated with the left heart system-related parameters BP ($R_f = 0.809$) and CO ($R_f = 0.745$). However, the coefficients for the right heart system-related parameters CVP and PAP were smaller than those of the left heart system-related parameters ($R_f = 0.643$ and 0.670, respectively) (Table 2).

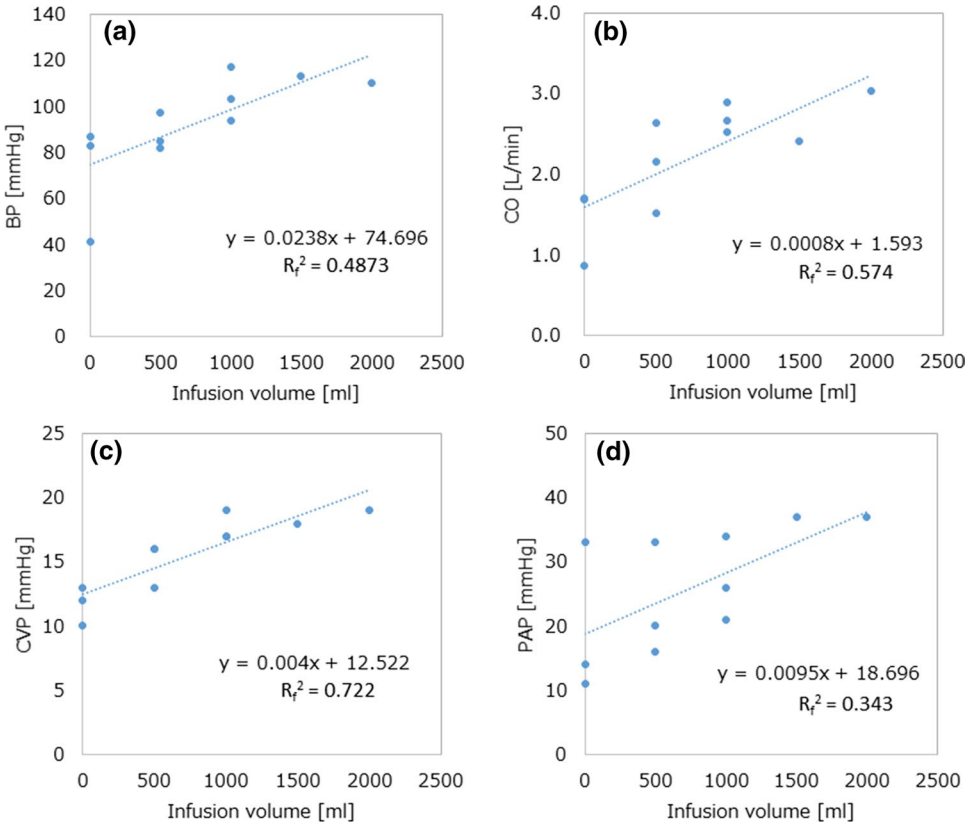

Fig. 3 Circulatory reactions to a fluid infusion between **a** blood pressure (BP) and the infusion volume, **b** cardiac output (CO) and the infusion volume, **c** central venous pressure (CVP) and the infusion volume, and **d** pulmonary arterial pressure (PAP) and the infusion volume

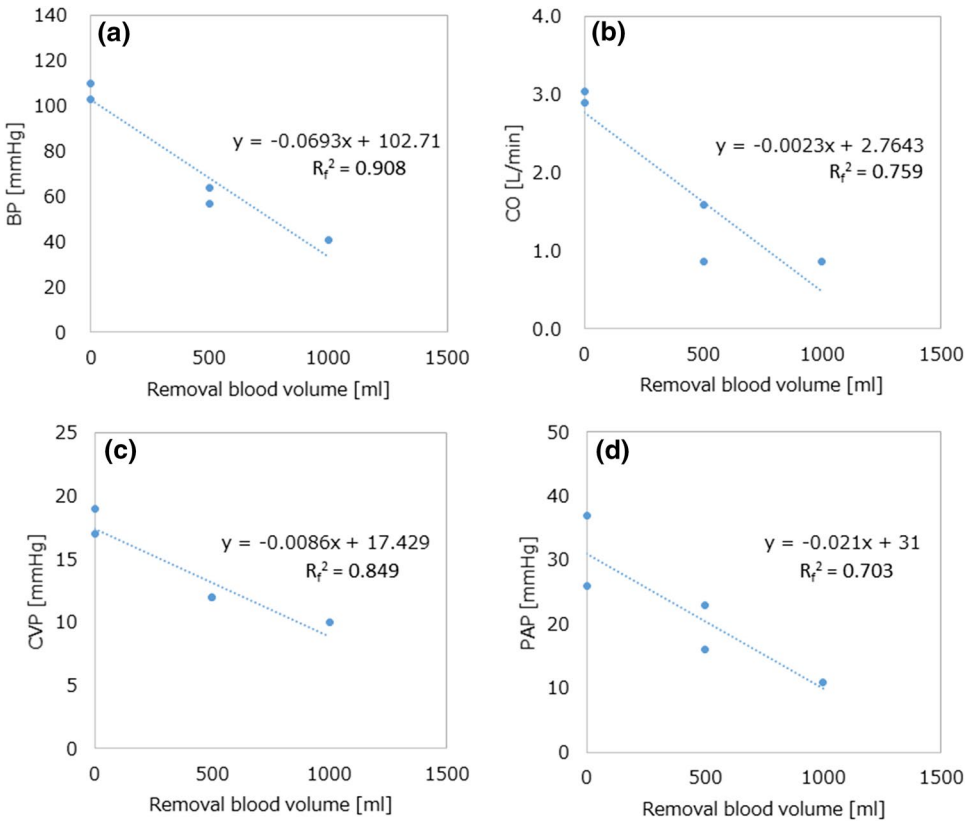

Fig. 4 Circulatory reactions to blood removal between **a** blood pressure (BP) and the blood removal volume, **b** cardiac output (CO) and the blood removal volume, **c** central venous pressure (CVP) and the blood removal volume, and **d** pulmonary arterial pressure (PAP) and the blood removal volume

Table 1 Relationship between image parameters and fluid loading

Fluid loading	Relative lung density		Relative heart area	
	R_f^2	R_f	R_f^2	R_f
Fluid infusion	0.672	−0.820	0.197	0.444
Blood removal	0.956	0.978	0.868	−0.932

R_f^2 Freedom-adjusted coefficients of determination, R_f Adjusted coefficients

4 Discussion

The cardiovascular parameters CVP and CO changed depending on the fluid loading type, indicating that circulating blood volume and cardiac pumping function increased after infusion and decreased after blood removal. In a porcine model with normal circulatory reactions under fluid loading, cardiovascular parameters showed a linear correlation with radiographic findings on dynamic chest radiographs. These results suggest that DCR has the diagnostic capacity to not only detect perfusion defects, as demonstrated in previous studies [6], but to also evaluate relative circulating blood volume and cardiac function.

In the infusion/blood removal experiments, radiographic lung density and the size of the heart shadow changed in response to the amount of fluid infusion and blood removal. Consequently, high linearity was confirmed between the fluid loading and image parameters. The decrease in radiographic lung density was caused by increased X-ray attenuation in the lungs and vice versa. Thus, our findings reflect the systemic fluid level. Qualitative studies have demonstrated that pulmonary overhydration causes low translucency in the vascular, interstitial, and alveolar phases on chest radiography in patients with chronic heart failure [19]. Wang et al. (2011) reported that the vascular pedicle width is correlated with overhydration, based on a meta-analysis [20]. These results indicate that the measurement of radiographic lung density with DCR allows for a relative evaluation of the fluid volume in the body.

Another notable observation was a linear correlation between the image parameters and the circulatory parameters CO, BP, CVP, and PAP. These results indicate that circulatory-physiological parameters can be estimated based on real-time DCR, which is useful for estimating changes in rapid systemic hydration in intensive care unit (ICU) patients during an operation. Heart failure could be detected as decreased temporal changes in radiographic density and/or relative heart size, and thus the use of a ventricular assist device should be considered based on the results of DCR. However, the relative heart size showed reduced

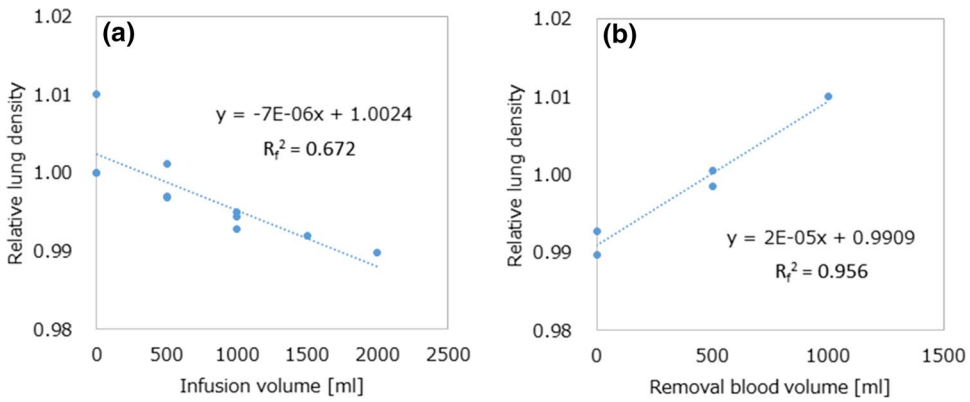

Fig. 5 Relationship between **a** the relative lung density and the infusion volume (R_f = 0.820) and **b** the relative lung density and the blood removal volume (R_f = 0.978)

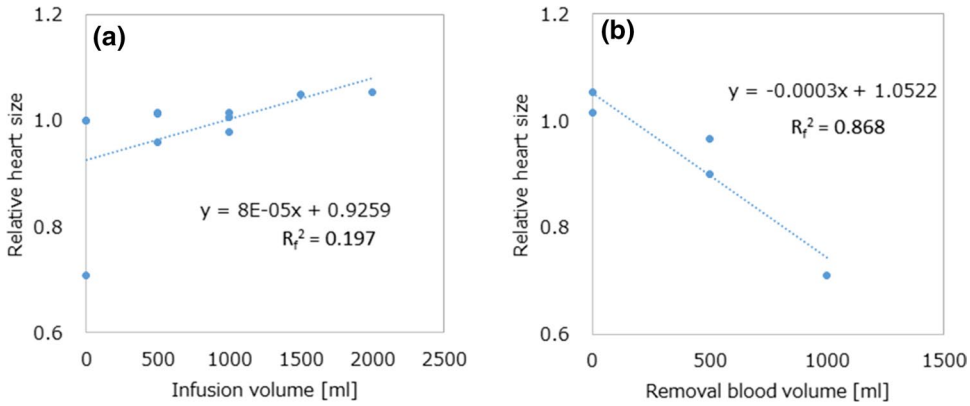

Fig. 6 Relationship between **a** the relative heart size and the infusion volume (R_f = 0.444) and **b** the relative heart size and the blood removal volume (R_f = 0.932)

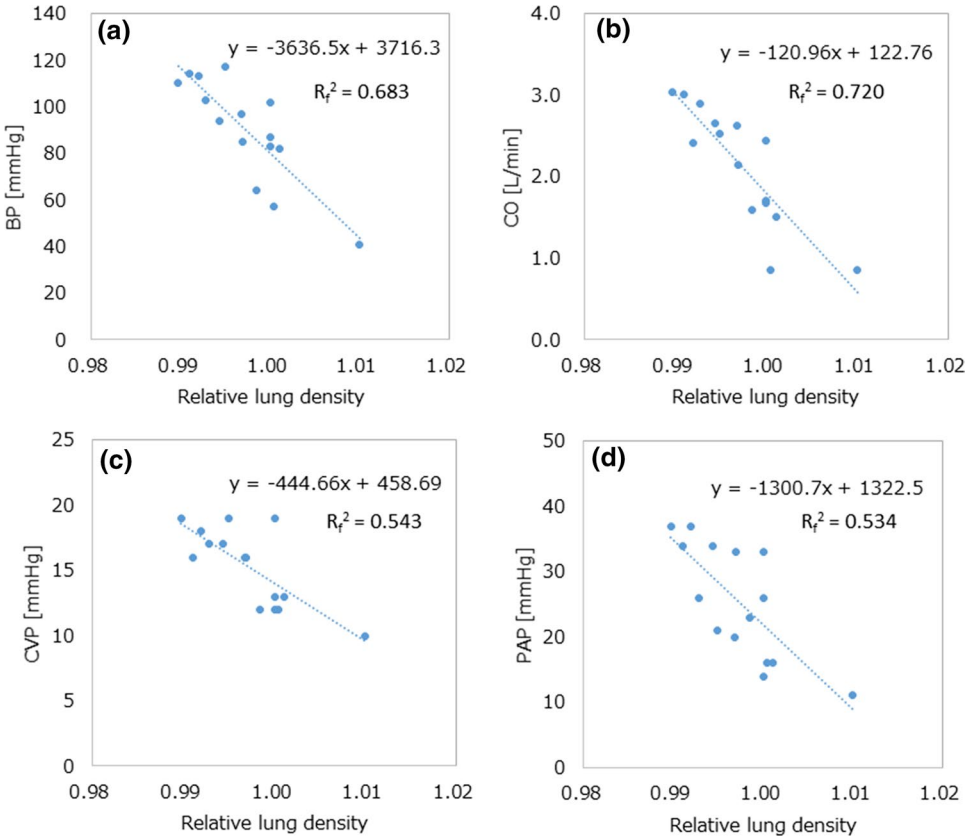

Fig. 7 Relationship between the relative lung density and **a** blood pressure (BP) (R_f = 0.827), **b** cardiac output (CO) (R_f = 0.848), **c** central venous pressure (CVP) (R_f = 0.737), and **d** pulmonary arterial pressure (PAP) (R_f = 0.731)

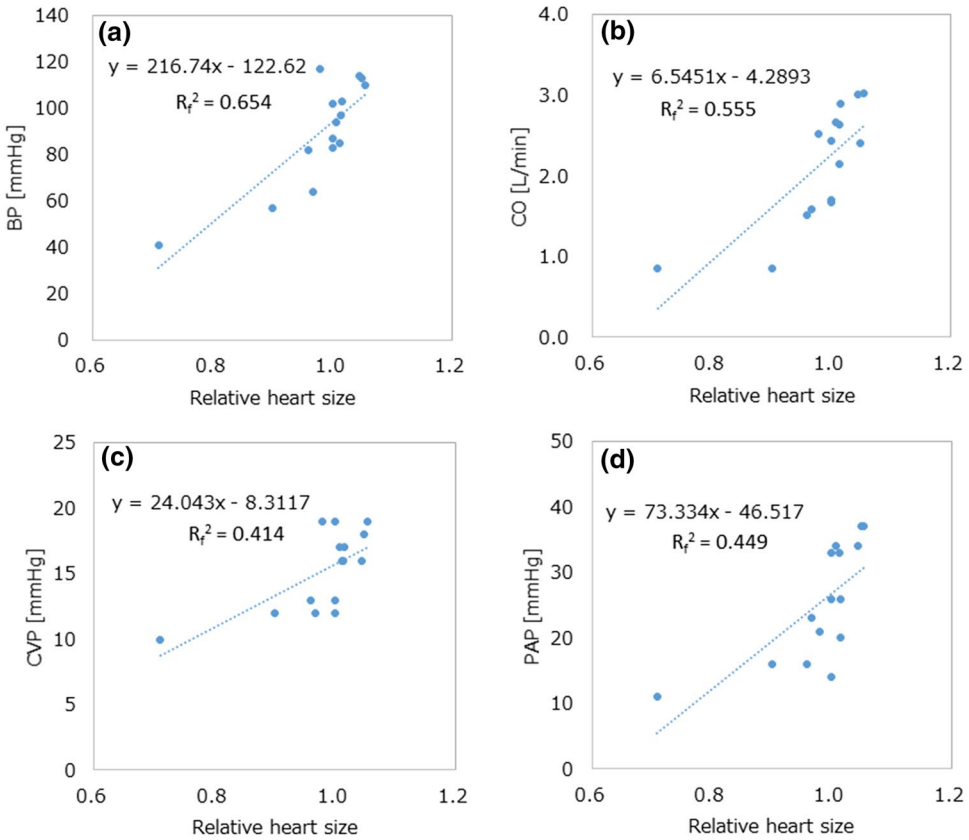

Fig. 8 Relationship between the relative heart size and **a** blood pressure (BP) (R_f = 0.809), **b** cardiac output (CO) (R_f = 0.745), (c) central venous pressure (CVP) (R_f = 0.643), and (d) pulmonary arterial pressure (PAP) (R_f = 0.670)

Table 2 Relationship between image and cardiovascular parameters

Circulatory parameters	Relative lung density		Relative heart area	
	R_f^2	R_f	R_f^2	R_f
BP	0.683	0.827	0.654	0.809
CO	0.720	0.848	0.555	0.745
CVP	0.543	0.737	0.414	0.643
PAP	0.534	0.731	0.449	0.670

BP blood pressure, *CO* cardiac output, *CVP* central venous pressure, *PAP* pulmonary artery pressure

R_f^2 Freedom-adjusted coefficients of determination, R_f Adjusted coefficients

correlations with the right heart system-related parameters (PAP and CVP). In the current study, image and circulatory parameters were evaluated within the first 5 min after fluid loading. This approach was adopted because of the rapid nature of in vivo responses to changes in fluid load, and the left heart system-related parameters exhibited stronger correlations with the image parameters than with the right heart system-related parameters. The reactions of the right heart system-related parameters were slow, and these parameters also took a relatively long time to stabilize. Therefore, further considerations for optimal measurement periods for right heart system-related parameters may be required.

The current study had some limitations. First, the measurements were performed in the lung or the whole heart unit; therefore, the sensitivity and spatial resolution of the present method for evaluating relative cardiovascular parameters remain to be fully determined. Second, the present technique compared values to the baseline values in the same subject. Third, in some cases, the image parameters reached a plateau after excessive fluid loading (fluid infusion/blood removal), highlighting one of the limitations of the DCR approach. Fourth, the number of porcine models used was small. Although the use of radiographic imaging parameters was confirmed in a porcine study under fluid loading, the target accuracy in estimating cardiovascular parameters remains to be determined. Further laboratory studies are required to confirm the diagnostic performance of the technique in conjunction with clinical studies involving many patients.

Although the present study was an animal study using four porcine models, the findings reveal the potential of DCR for the evaluation of cardiovascular conditions based on radiographic findings. DCR can be performed using a similar procedure as that used for conventional chest radiography. Moreover, to facilitate visual evaluation, slight changes in radiographic density can be visualized in the form of a color display, that is, as changes in color scale [2, 6, 7, 9]. Although the lung and heart regions were manually determined in this experimental study, they were determined using an automatic lung segmentation technique [21]. Such a physiological and functional radiography technique is applicable for ICU patients who require rapid examination, as well as for those who require follow-up examinations and postoperative management. As portable dynamic FPD systems have been released, they will conceivably become available in patient rooms, ICUs, and emergency rooms.

In conclusion, we confirmed a high correlation between cardiovascular and image parameters obtained using DCR. Our findings indicate that relative cardiovascular parameters can be evaluated based on image parameters such as the size of the heart shadow and radiographic lung density. DCR is expected to be a simple and rapid diagnostic tool for providing radiographic image information and estimating circulatory parameters in emergency settings.

Supplementary Information The online version contains supplementary material available at https://doi.org/10.1007/s12194-021-00626-2.

Funding This research was supported in part by a grant-in-aid program for revitalization in Fukushima, Japan.

Declarations

Ethical adherence This study was approved by the Institutional Animal Care and Use Committee of Shiga University of Medical Science. All animal experiments complied with the ARRIVE guidelines and were carried out in accordance with the U.K. Animals (Scientific Procedures) Act, 1986 and associated guidelines, EU Directive 2010/63/EU for animal experiments.

References

1. Karim B, Chris F, Simon H, Heather J, Richard L, Simon Mc. Major trauma: Assessment and initial management. National Clinical Guideline Centre. NICE Guideline No. 39, 2016.
2. Tanaka R. Dynamic chest radiography: flat-panel detector (FPD) based functional X-ray imaging. Radiol Phys Technol. 2016;9(2):139–53. https://doi.org/10.1007/s12194-016-0361-6.
3. Sanada S. Functional dynamic radiology with computer analysis for physiological chest imaging and kinematic joint imaging. Quant Imaging Med Surg. 2017;7(6):698–706. https://doi.org/10.21037/qims.2017.12.01.
4. Annex IV. Schedule III. Guidance levels of dose, dose rate and activity for medical exposure. In: Radiological Protection for Medical Exposure to Ionizing Radiation. Safety Guide. IAEA Safety Standards Series No. SSG-46. Vienna: International Atomic Energy Agency (IAEA), 2018.
5. Miyatake H, Fujino K, Tabata T, Tsujita Y, Tanaka R, and Eguchi Y. Detection of pulmonary embolism using a novel dynamic flat-panel detector system in monkeys. Circ J 2021 (In press).
6. Tanaka R, Tani T, Nitta N, Tabata T, Matsutani N, Muraoka S, et al. Detection of pulmonary embolism based on reduced changes in radiographic lung density during cardiac beating using dynamic flat-panel detector: an animal-based study. Acad Radiol. 2019;26(10):1301–8. https://doi.org/10.1016/j.acra.2018.12.012.
7. Tanaka R, Sanada S, Fujimura M, Yasui M, Tsuji S, Hayashi N, et al. Development of pulmonary blood flow evaluation method with a dynamic flat-panel detector (FPD): quantitative correlation

analysis with findings on perfusion scan. Radiol Phys Technol. 2010;3(1):40–5. https://doi.org/10.1007/s12194-009-0074-1.
8. Tanaka R, Sanada S, Fujimura M, Yasui M, Tsuji S, Hayashi N, et al. Pulmonary blood flow evaluation using a dynamic flat-panel detector: Feasibility study with pulmonary diseases. Int J Comput Assist Radiol Surg. 2009;4(5):449–54. https://doi.org/10.1007/s11548-009-0364-4.
9. Tanaka R, Sanada S, Fujimura M, Yasui M, Nakayama K, Matsui T, et al. Development of functional chest imaging with a dynamic flat-panel detector (FPD). Radiol Phys Technol. 2008;1(2):137–43. https://doi.org/10.1007/s12194-008-0020-7.
10. Yamazaki Y, Abe K, Hosokawa K, Kamitani T. A novel pulmonary circulation imaging using dynamic digital radiography for chronic thromboembolic pulmonary hypertension. Eur Heart J. 2020;41(26):2506. https://doi.org/10.1093/eurheartj/ehaa143.
11. Hanaoka J, Yoden M, Hayashi K, Shiratori T, Okamoto K, Kaku R, Kawaguchi Y, Ohshio Y, Sonoda A. Dynamic perfusion digital radiography for predicting pulmonary function after lung cancer resection. World J Surg Oncol. 2021;19(1):43.
12. Yamazaki Y, Hosokawa K, Tsutusi H, Ishigami K. Pulmonary ventilation–perfusion mismatch demonstrated by dynamic chest radiography in giant cell arteritis. European Heart Journal, ehaa443, https://doi.org/10.1093/eurheartj/ehaa443, 2020.
13. Tanaka R, Matsumoto I, Tamura M, Takata M, Kasahara K, Ohkura N, Inoue D, Matsuura Y. Comparison of dynamic flat-panel detector-based chest radiography with nuclear medicine ventilation-perfusion imaging for the evaluation of pulmonary function: a clinical validation study. Med Phys. 2020. https://doi.org/10.1002/mp.14407.
14. Squire LF, Novelline RA. Fundamentals of Radiology. 4th ed. Cambridge, Massachusetts, and London: Harvard University; 1988.
15. Hansen JT, Koeppen BM. Cardiovascular Physiology, In: Netter's Atlas of Human Physiology (Netter Basic Science). Icon Learning Systems: Teterboro, New Jersey; 2002.
16. Kvalseth TO. Cautionary note about R^2. The American Statitian. 1985;39:279–85.
17. Taylor R. Interpretation of the correlation coefficient: a basic review. J Diagn Med Sonography. 1990;6(1):35–9.
18. Gullford JP. Fundamental Statistics in Psychology and Education. New York: McGraw-Hill Book Company; 1977.
19. Moses S. Chest XRay in Congential Heart Failure. Cardiovascular Medicine Book, FPnotebook. https://fpnotebook.com/cv/Rad/ChstXryInCngntlHrtDs.htm Accessed Jan 11, 2020.
20. Wang H, Shi R, Mahler S, Gaspard J, Gorchynski J, D'Etienne J, et al. Vascular pedicle width on chest radiography as a measure of volume overload: meta-analysis. West J Emerg Med. 2011;12(4):426–32. https://doi.org/10.5811/westjem.2011.3.2023.
21. Kitahara Y, Tanaka R, Roth H, Oda H, Mori K, Kasahara K, et al. Lung segmentation based on a deep learning approach for dynamic chest radiography. Proc. of SPIE 10950, Medical Imaging 2019: Computer-aided diagnosis, 109503M-1–7. https://doi.org/10.1117/12.2512711.

Publisher's Note Springer Nature remains neutral with regard to jurisdictional claims in published maps and institutional affiliations.